Effect of Dielectric Film Thickness on Dielectric Charging of RF MEMS Capacitive Switches

R. Daigler[1], G. Papaioannou[2], E. Papandreou[2], and J. Papapolymerou[1],

[1] School of ECE, Georgia Institute of Technology, Atlanta, GA, 30332-0250, USA
[2] University of Athens, Physics Department., Solid State Physics Section, , Athens, 15784

***Abstract* — For the first time, the effects of dielectric film thickness in the dielectric charging process of RF MEMS capacitive switches is presented. Both MEMS switches and MIM capacitors are used to investigate charging phenomena. The contribution of charge injection and dipole orientation has been identified. An empirical law that allows the prediction of stored charge on the film thickness was drawn. Above room temperature, the dependence of thermally stimulated depolarization current on a certain activation energy that is independent of dielectric film thickness allows the inclusion of this behavior in modeling tools.**

***Index Terms* — Dielectric materials, microelectromechanical devices, MIM devices, reliability.**

I. Introduction

RF MEMS switches are one of the most promising applications in microelectromechanical systems (MEMS), but their commercialization is hindered by reliability problems. The most important problem is the charging of the dielectric, causing erratic device behavior [1]-[4]. Presently, the available models assume that the dielectric charging arises from charges distributed throughout the dielectric material [4], the presence of charges at the dielectric interface [5], and the injection of charges from the suspended bridge during ON-state [6]. So far the dielectric charging process has been investigated by recording the transient current in permanently ON switches [7]-[10], the transient response of the ON capacitance [11]-[12], and the correlation of Poole-Frenkel current intensity to the shift of pull-out voltage [9]. The simultaneous study of dielectric charging by recording the capacitance voltage characteristic in capacitive switches and the thermally stimulated depolarization current (TSDC) in metal-semiconductor-metal (MIM) structures, with the same dielectric, has been proposed recently [13]. This method allows both the determination of the main contributing charging mechanisms, which are charge injection and dipole orientation. The effect of temperature on dielectric charging has been investigated in MIM capacitors with silicon oxide (SiO_2) dielectric [7]-[9] and in MEMS switches with silicon nitride (Si_3N_4) dielectric [11]-[12]. Finally, a process arising from contactless charging and related to the dielectric intrinsic polarization processes has been reported [14]-[15].

These efforts constitute a major step towards the understanding of MEMS dielectric charging but have not yet been associated with parameters such as the dielectric film thickness and the deposition method. The aim of the present work is to investigate the effect of dielectric film thickness on the charging processes. In order to realize this, both MEMS switches and MIM capacitors are employed. The investigation is based on recording the capacitance-voltage characteristic in MEMS switches and applying the TSDC method on MIM capacitors.

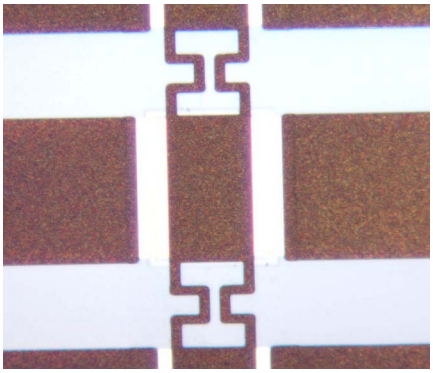

Fig. 1. Top view of a shunt RF MEMS capacitive switch.

II. Experimental Analysis

Fig. 1 depicts a RF MEMS capacitive switch utilized in this experiment. The switches were fabricated with a standard photolithographic process on high resistivity silicon wafers (>10k -cm). The dielectric film is PECVD Si_3N_4 deposited at 150°C. Switches with 200 nm and 430 nm dielectrics were fabricated The membrane is an evaporated titanium-gold seed layer electroplated to a thickness of 2 μm. Under no applied force, the membrane is normally suspended 2 μm above the dielectric. The sacrificial layer was removed with resist stripper and the switches were dried using a critical point dryer.

Capacitance voltage (CV) characteristics were performed for the RF MEMS switches. The capacitance was monitored with a Boonton 72B capacitance meter while sweeping the voltage in .5 V steps in the temperature range of 300K to 450K. Assuming

$$E = \frac{V}{d}, \tag{1}$$

TABLE I
MIM LAYER STRUCTURE

Layer	Symmetric	Asymmetric
Au	200nm	200nm
Ti	20nm	20nm
Si_3N_4	100nm – 600nm	100nm – 600nm
Ti	20nm	-
Au	200nm	200nm
Ti	20nm	20nm
Si	500µm	500µm

where d is the thickness of the dielectric, the maximum voltage when performing the CV characteristic for the 430 nm thick dielectric case has been chosen to be twice that of the 200 nm thick dielectric case to provide approximately a constant electric field across both dielectrics.

MIM capacitors have been fabricated in an analogous way to the RF MEMS switches. The dielectric film is PECVD Si_3N_4 deposited at 150°C. Capacitors with dielectric film ranging from 100 nm to 600 nm and symmetrical or asymmetrical contacts have been fabricated. Table I lists the different MIM layer structures. The charging process was investigated by applying the TSDC method presented in [16]. This allowed the calculation of stored charge, the analysis of various charging mechanism and their dependence on the film thickness, bias polarity, and metal insulator contacts. The TSDC current was measured with a Keithely 6487 voltage source-picoampere meter in the temperature range of 200K to 450K. The polarization bias was adjusted for each MIM capacitor to ensure a constant electric field of 1 MV/cm for all samples. Finally, the heating rate was =2.5 K/min.

III. RESULTS AND DISCUSSIONS

A. MIM Capacitors

In insulators, the time and temperature dependence of polarization and depolarization processes are, in the case of dipolar polarization, determined by the competition between the orienting action of the electric field and the randomizing action of thermal motion. The depolarization process in a MIM capacitor will induce a short circuit discharge current transient (DCT) that is given by

$$I_{dis}(t) = -\frac{dP(t)}{dt} = \frac{P(t)}{\tau}. \qquad (2)$$

Moreover, the current density produced by the progressive decrease in polarization in the course of TSDC experiment, where time and temperature are simultaneously varied, is approximated by

$$J_D(T) \approx \frac{P_S(T_p)}{\tau_0} \cdot \exp\left(-\frac{E_A}{kT}\right) \cdot \exp\left[-\frac{1}{\beta\tau_0} \cdot \frac{kT^2}{E_A} \exp\left(-\frac{E_A}{kT}\right)\right] \qquad (3)$$

where is the heating rate (K/sec), E_A is the depolarization mechanism activation energy, P_S (T_P) is the equilibrium polarization at the polarizing temperature T_P, and $_O$ is the corresponding infinite temperature relaxation time.

In the case of space charge polarization induced by charge injection, the processes leading to thermally stimulated depolarization current are far more complex because several mechanisms such as the counteracting action of diffusion, the loss of migrating carriers due to recombination, the blocking effect of the electrode-dielectric interfaces, the charge trapping, and the influence of local electric fields can be involved simultaneously. Under these circumstances the TSDC spectra show the characteristic properties of distributed processes, such as extension over a wide temperature range. In addition, only a part of the space charge decay is monitored in the MIM capacitors current as a consequence of the partial dissipation of excess charges by space independent intrinsic conductivity, the incomplete release of the image charges induced at the electrodes, and the dependence of the diffusion released current on the blocking character of the electrodes [16]. A typical TSDC spectrum is show in Fig. 2. The application of (3) allows partial analysis of the spectrum at temperatures above 300K. At lower temperatures, the spectrum cannot be analyzed and this behavior has to be attributed to charging induced by injected charges.

Since the heating rate is constant, the TSDC spectrum allows the calculation of stored charge:

$$\sigma = \frac{1}{\beta A}\int_{T1}^{T2} I_{TSDC}(T)dT \cdot \qquad (4)$$

where A is the capacitor area. The dependence of stored charge on film thickness is presented in Fig. 3. Assuming that in the absence of dielectric there must be no stored charge, we can draw an empirical equation for the dependence of the stored charge on the dielectric thickness,

$$\sigma(d) = \sigma_0 \cdot d^{\gamma}. \qquad (5)$$

The fitting of (5) to experimental data gave $_O$=0.067 C/cm^2 and =0.58. Since (5) is an empirical equation, further work is

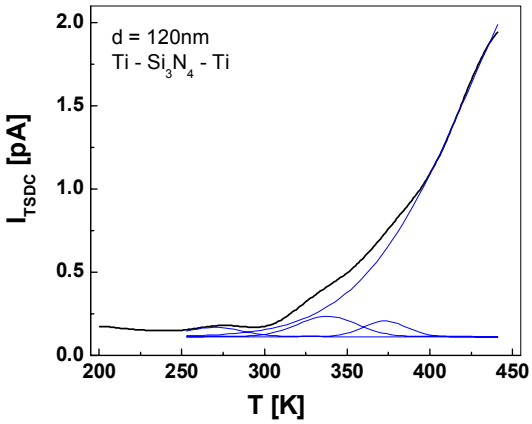

Fig. 2. Typical TSDC spectrum.

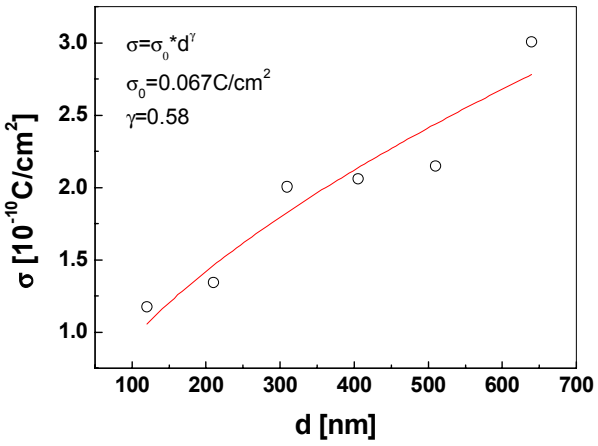

Fig. 3. Dependence of total stored charge on film thickness.

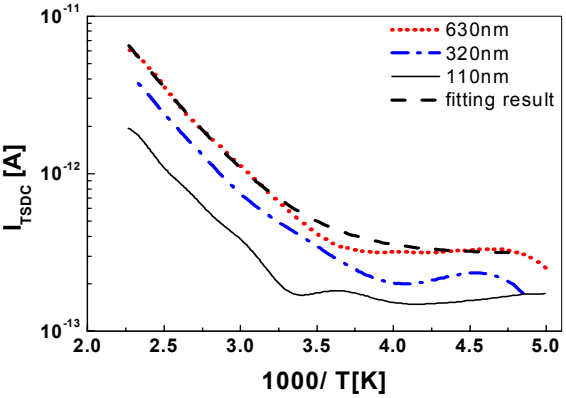

Fig. 4. Temperature dependence of TSDC spectrum.

continuing in order to derive a model based on physical parameters. Here it must be pointed out that (5) was found to be independent on the nature of applied contacts. Finally the TSDC spectra for all MIM capacitors reveal a common behavior; above room temperature the TSDC current is thermally activated (Fig. 4)

$$I_{TSDC}(T) = I_1 + I_0 \exp\left(-\frac{E_A}{kT}\right). \quad (6)$$

The fitting of (6), which includes the Arrhenius plot of the thermally activated part, to the experimental data of the 630 nm MIM capacitor, reveals activation energy of 0.25 eV and current levels of 3.1×10^{-13} A for I_1 and I_0 respectively. It should be noted that similar activation energy was obtained for all samples. This common behavior, which is independent of dielectric film thickness, leads us to the conclusion that it can be included in modeling tools of dielectric charging.

In order to examine the universality of the power law behavior, we plotted the value r, the normalized TSDC current with respect to its value for the 630 nm MIM capacitor, and calculated at four different temperatures. The temperatures were selected to include the region of polarization induced by charge injection, the onset of dipole induced polarization, and two temperatures where the dipole orientation is the leading charging mechanism. The fitting was performed using a power law equation, similar to (5), with a fixed value of =0.58. Fig. 5 shows the fitting result that seems to agree reasonably well with the experimental data. Here it must be pointed out that the fitting was performed by taking into account all data in (6), which is data for all temperatures. The last step allows us to assume that we can approximate the TSDC current dependence on temperature and dielectric film thickness through

$$I_{TSDC}(T,d) = r_0 \cdot d^{\gamma} \cdot \left[I_1 + I_0 \cdot \exp\left(-\frac{E_A}{kT}\right) \right]. \quad (7)$$

Due to the significance of this result the investigation is presently extended to dielectric films that are deposited at different temperatures.

B. RF MEMS

The capacitance-voltage descending voltage minimum variation with temperature is thermally activated too. This arises from the fact that the voltage minimum (Vmin) is proportional to the dielectric stored charge

$$Vmin = \frac{\sigma d}{\varepsilon_0} \quad (8)$$

The voltage minimum shift was fitted with a function similar to (6). The excellent fitting result with V_0=-1.22 V and an activation energy of 0.40 eV is presented in Fig. 6. The higher activation energy may be attributed to the fact that in MIM capacitors the top electrode is deposited by evaporation while the dielectric charging in a MEMS switch occurs through mechanical contact through a rough surface that is present on both the dielectric surface, due to electroplated membrane, and the contacting bridge, due to sacrificial layer.

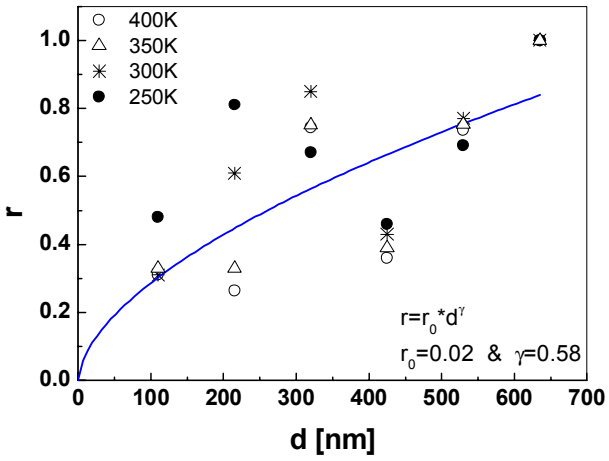

Fig. 5. Normalized TSDC current ratio with respect to 630 nm dielectric film.

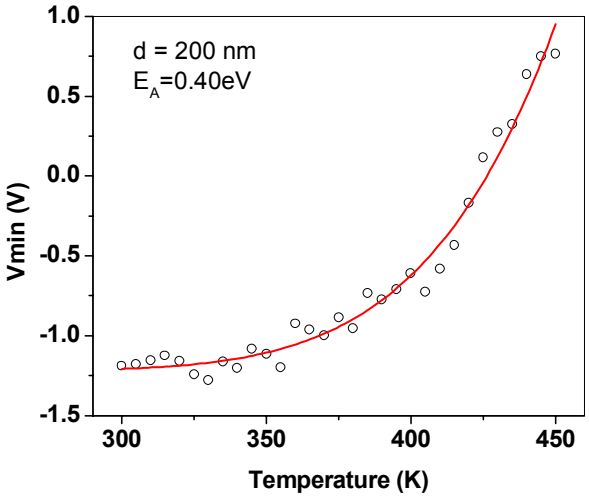

Fig. 6. CV descending voltage min. variation with temperature.

IV. Conclusion

The dependence of charging mechanisms on the dielectric film thickness has been investigated. The study was performed by employing RF MEMS capacitive switches with 200 nm and 430 nm thick Si_3N_4 and MIM capacitors with 100nm to 650nm Si_3N_4. The contribution of charge injection and dipole orientation has been identified. An empirical law that allows the prediction of stored charge on the film thickness was drawn. Finally, above room temperature the dependence of the thermally stimulated depolarization current on a certain activation energy that is independent of dielectric film thickness allows the inclusion of this behavior in modeling tools.

Acknowledgements

This work was partially supported by the IMPACT Center for Advancement of MEMS/NEMS VLSI, funded by DARPA, through Grant No. HR0011-06-1-0046, under the DARPA N/MEMS Science and Technology Fundamentals Research Program, and partially by the Hellenic GSRT in the frame of Scientific and Technological Cooperation between TRD Organizations in Greece and RTD Organizations in U.S.A. under the contract No. 05-NON-EU-212

References

C. L. Goldsmith, J. Ehmke, A. Malczewski, B. Pillans, S. Eshelman, Z. Yao, J. Brank, and M. Eberly, "Lifetime characterization of capacitive RF MEMS switches," *IEEE MTT-S Int. Microwave Symp, Dig.,* pp.227-230, 2001.

[2] J. Wibbeler, G. Pfeifer, and M. Hietschold, "Parasitic charging of dielectric surfaces in capacitive microelectromechanical systems (MEMS)," *Sensors Actuators*, vol. A 71, pp.74-80, 1998.

[3] X. Yuan, S. Cherepko, J. Hwang, C. L. Goldsmith, C. Nordquist, and C. Dyck, "Initial observation and analysis of dielectric-charging effects on RF MEMS capacitive switches," *IEEE MTT-S Int. Microwave Symp, Dig.,* pp.1943-1946, 2004.

[4] G. M. Rebeiz, *RF MEMS Theory, Design and Technology*, Haboken, New Jersey: J. Willey and Sons, 2003.

[5] W. M. van Spengen, R. Puers, R. Mertens, and I. de Wolf, "A comprehensive model to predict the charging and reliability of capacitive RF MEMS switches," *J. Micromech. Microeng*.., vol. 14, pp. 514-521, 2004.

[6] X. Rottenberg, B. Nauwelaers, W. De Raedt, and H. A. C. Tilmans, "Distributed dielectric charging and its impact on RF MEMS devices," *12th GAAS Symposium*, pp.475-478, 2004.

[7] X. Yuan, J. C. M. Hwang, D. Forehand, and C. L. Goldsmith, "Modeling and characterization of dielectric-charging effects in RF MEMS capacitive switches," *IEEE MTT-S Int. Microwave Symp. Digest, pp.753-756* , 2005.

[8] S. Melle, D. De Conto, L. Mazenq, D. Dubuc, B. Poussard, C. Bordas, K. Grenier, L. Bary, O. Vendier, J.L. Muraro, J.L. Cazaux, and R. Plana, "Failure predictive model of capacitive RF-MEMS," *Microelectronics Reliability*, vol. 45, pp.1770-1775, 2005.

[9] X. Yuan, Z. Peng, J. C. M. Hwang, D. Forehand, and C. L. Goldsmith, "Temperature acceleration of dielectric charging in RF MEMS capacitive switches ," *IEEE MTT-S Int. Microwave Symp. Dig*., pp. 47-50, 2006.

[10] M.Lamhamdi, J.Guastavino, L.Boudou, Y.Segui, P.Pons, L. Bouscayrol, and R. Plana, "Charging effects in RF capacitive switches influence of insulating layers composition," *Microelectronics Reliability*, vol. 46, pp.1700–1704, 2006.

[11] G. J. Papaioannou, M. Exarchos, V. Theonas, G. Wang, and J. Papapolymerou, "Temperature study of the dielectric polarization effects of capacitive RF MEMS switches," *IEEE Transactions on Microwave Theory and Techniques*, vol. 53, pp.3467-3473, 2005.

[12] G. J. Papaioannou, M. Exarchos, V. Theonas, J. Psychias and G. Konstantinidis, D. Vasilache, A. Muller, and D. Neculoiu, "Effect of space charge polarization in radio frequency microelectromechanical system capacitive switch dielectric charging," *Appl. Physics Letters*, vol. 89, pp. 103512-4, 2006.

[13] G. Papaioannou, J. Papapolymerou, P. Pons, and R. Plana, "Dielectric charging in radio frequency micro-electro-mechanical-system capacitive switches: a study of material properties and device performance," *Applied Physics Letters*, vol. 90, pp.2335071-3, 2007.

[14] P. Czarnecki, X. Rottenberg, R. Puers, and I. De Wolf, "Effect of gas pressure on the lifetime of capacitive RF MEMS switches," *MEMS-2006, 19th International Conference on Micro Electro Mechanical Systems*, pp.890-893, 2006.

[15] G. J. Papaioannou, G. Wang, D. Bessas, and J. Papapolymerou, "On the polarization mechanisms of RF MEMS capacitive switches," *1st EuMIC Conference,* Manchester, pp.513-516, 2006.

[16] J. Vandershueren and J. Casiot J, in: P. Braunlich (Ed.), *Topics in Applied Physics: Thermally stimulated Relaxation in Solids,* vol. 37, ch.4, pp 135-223, Springer-Verlag, Berlin, 1979.